# A Modular UHF Reader Frontend for a Flexible RFID Testbed

Robert Langwieser, Gregor Lasser, Christoph Angerer,
Markus Rupp, and Arpad L. Scholtz

Institute of Communications and Radio-Frequency Engineering,
Vienna University of Technology
Gusshausstrasse 25/389, 1040 Wien, Austria
{robert.langwieser,gregor.lasser,christoph.angerer,
markus.rupp,arpad.scholtz}@nt.tuwien.ac.at,
http://www.nt.tuwien.ac.at

**Abstract.** Currently RFID (radio frequency identification) technology is pushing to the market mainly forced by industry. Passive tags in the UHF (ultra high frequency) region are of particular interest e.g. for supply chains, showing a tendency to become state of the art. Passive tags obtain their energy from the readers during communication. The reader has to power the tag by radiating energy at the same time as it has to receive the tag answer. Due to this so-called self-interference the reader frontend design becomes more complex than that of typical communication systems. In this paper we present the implementation of a modular UHF reader frontend for a flexible RFID testbed.

**Key words:** RF-Engineering, RFID, Reader, Testbed, Frontend, Rapid Prototyping

## 1 Introduction

A simple RFID (radio frequency identification) scenario consists of a reader and a transponder. The latter is also termed the tag. Communication between the reader and the tag is bidirectional. The tag can answer specific commands sent by the reader. RFID systems can be categorized in various ways e.g. frequency range, read range, near field or far field communication. Additionally, transponders can be divided with respect to their power supply into three types: active tags, semi-active tags or passive tags [1]. Active tags have an internal power supply and require no additional external power. The internal power supply is used for their integrated circuits as well as for the transmission to the reader. Read range and lifetime depend on the internal power supply. Semi-passive tags also have an onboard power supply but this is only used for supplying the integrated circuits and not used for powering the radio transmission. For this kind of tags the tag answers by reflecting or backscattering a part of the RF (radio frequency) energy transmitted by the reader [2]. Lifetime of such tags depends again on the internal power supply. For a fixed transmit power of the reader the read range is depending either on the reader sensitivity or on the tag sensitivity. Passive tags have no internal power supply and are powered only by the energy emitted by the reader. Backscattering is used by the tag for communication. Such tags rectify the received RF energy for powering their circuits. In this case the range limitation for a fixed transmit power of the reader is determined on the one hand by the power consumption of the tag and on the other hand by the energy transformation efficiency of the tag.

The different types of tags define also different requirements for the reader. In the cases of a semi-active or of a passive tag the design of a reader frontend differs most from a common RF frontend design due to the self-interference during the tag answer. Currently (and probably also in the future) the passive tag in the UHF domain is the most popular tag type, due to its low cost and large read range capabilities. The frequency used is 868 MHz in Europe and 915 MHz in North America,

The passive transponder technology available in the UHF region changes rapidly due to an evolutionary process forced by the chip designers and by new tag antenna designs. Currently read range and tag complexity is limited by the power supply of the tag. Therefore, in further chip designs power consumption of the tags is minimized and at the same time the rectifiers of the tags become more efficient. This leads to larger communication distances between reader and tag. Accordingly, the system limitation with respect to the read range will be shifted more and more from the tags wake up power to the sensitivity of the reader. Additionally, standardization is ongoing and requires changes to e.g. protocols, modulation scheme and transmit power.

In order to tackle these problems we have implemented a flexible and rapidly reconfigurable RFID test environment. This testbed is designed to support several different RFID standards in two frequency ranges, the 13.56 MHz HF as well as the 868 MHz UHF frequency domain [3]. The RF frontend design presented in this paper is flexible in order to allow for a wide range of different experiments and testbed configurations. Furthermore, it is modular and expandable for future experiments, like beamforming techniques using several antennas or exploration of additional frequency ranges (2.4 GHz).

The rest of the paper is organised as follows: The next section gives an overview of the RFID testbed, while the following sections focus on the RF frontend for the RFID system. Section 3 describes the concept of the frontend as well as the receiver and transmitter in detail. Section 4 presents the verification results of the frontend, while the last section concludes the paper.

## 2 The RFID Testbed

Figure 1 depicts the basic structure of the RFID testbed. The main reconfigurable components are a fixed-point DSP from Texas Instruments (TMS320C6416) and a Xilinx Virtex II FPGA. Additionally, the testbed contains two digital to analog converters (16 bits) and two analog to digital converters (14 bits). An Ethernet interface connects the DSP to a PC thus allowing for communicating with an external application running on a PC. The testbed hardware, consist-

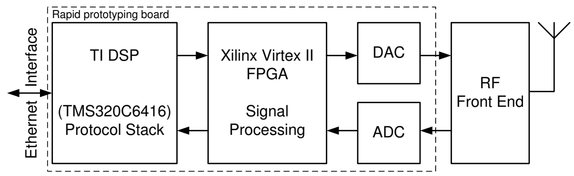


**Fig. 1.** Block diagram of the RFID testbed

ing of a rapid prototyping board [4] and an analog frontend, is selected to be independent from a specific standard or implementation. Hence, both the protocol stack and the signal processing parts are mapped to the DSP and FPGA available at the board, respectively. Also the RF frontend is flexible in terms of various parameters applicable in RFID systems, e.g. modulation schemes, different timings and signal bandwidths.

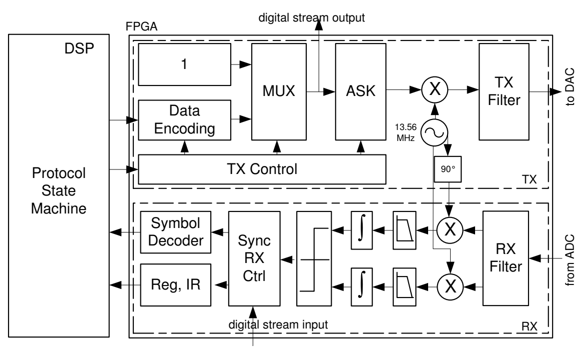


**Fig. 2.** FPGA architecture of the RFID testbed

A generic architecture that supports the EPC global standard in the HF [5] and UHF domain [6] as well as the ISO15693 [7] standard is shown in Figure 2. The transmitter is composed of the DSP to FPGA interface, a symbol encoder, a transmit state machine, the multiplexer to switch to continuous carrier mode, a modulator, upconverter to 13.56 MHz and finally the transmit filter. In case of an implementation in the UHF frequency domain the output signal is further up- and downconverted to 868 MHz in the RF frontend. The signal sampled at the receiver is also centered at 13.56 MHz in the ADC. Thereafter, it is first bandpass filtered to reduce the noise bandwidth, downconverted using an IQ demodulator, integrated and, finally the bits are detected using an algorithm that adapts its threshold according to the channel conditions [8]. Finally the decided levels are synchronised, the symbols decoded and forwarded to the DSP.

Different test scenarios on various levels, e.g. on the protocol stack and the signal processing algorithms, are carried out. This includes for example anticollision scenarios [9] and complex application scenarios like the inventory of all tags in the read range, as well as tracking the effects of different receiver architectures, with different demodulators or signal detection schemes for instance.

## 3 UHF Frontend

### 3.1 Frontend Concept

The concept and design for the transmitter and the receiver of the UHF frontend is flexible and only uses components off-the-shelf. In difference to a common wireless communication frontend an additional module, the CCU (carrier compensation unit), was added for canceling the self-interference or direct coupling at the receiver [10]. A microcontroller unit is part of the system concept for monitoring and control purposes as well as for possible communication with the rapid prototyping board for further applications. For operation in rather static scenarios the microcontroller is not required. In Figure 3 the frontend concept is illustrated.

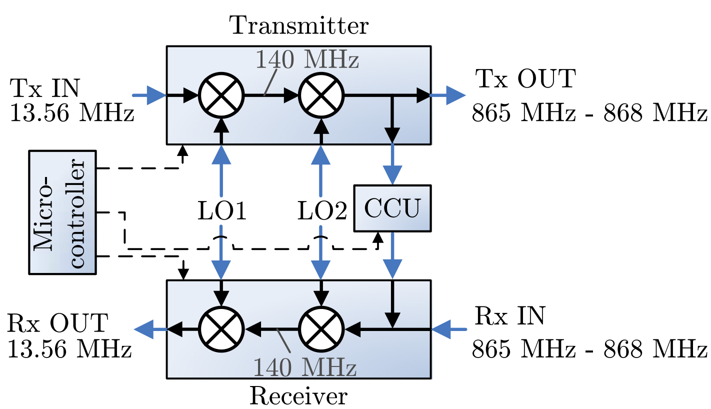


**Fig. 3.** Simplified block diagram of the UHF transmitter

Both transmitter and receiver are based on a low intermediate frequency (IF) to RF concept combined with a two stage frequency conversion [11]. Therefore, two local oscillator signals are required, which are provided by standard laboratory signal generators. The UHF frontend can be directly interlinked with the DSP/FPGA board at a frequency of 13.56 MHz. The analog frontend is not limited to the modulation schemes presently standardized for RFID due to the fact that modulation and demodulation as well as pulse shaping are performed by the DSP/FPGA board. The frontend performs as a linear transponder and can be used in a bi-static antenna scenario as well as in a mono-static antenna scenario. In a bi-static antenna scenario transmitter and receiver each have a separate antenna. For the mono-static scenario one common antenna is shared by the transmitter and the receiver. When the frontend is configured for a single antenna RFID reader scenario a circulator is required to provide decoupling between transmitter and receiver. For further improvement of transmitter-receiver isolation active carrier compensation is implemented.

### 3.2 Transmitter

The input interface of the transmitter is designed for a frequency of 13.56 MHz and a nominal input power of -10 dBm. To provide some enforced matching and to give an opportunity to adapt the frontend to higher input signal levels a fixed attenuator can be enabled as first element at the input. The first selective component is a lowpass filter with a 3 dB corner frequency of 30 MHz as shown in the simplified block diagram of the transmitter in Figure 4. The lowpass filter

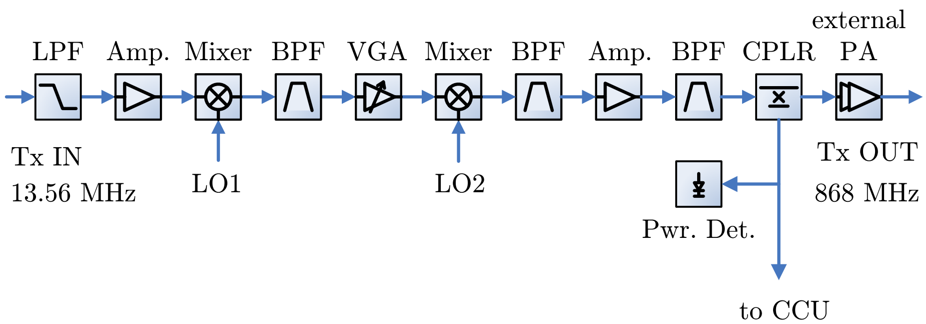


**Fig. 4.** Simplified block diagram of the UHF transmitter

in combination with the bandpass filter on the second IF provides suppression of undesired signals produced by the DAC of the rapid prototyping board. An amplifier compensates for the losses in the previous stages and provides isolation between the lowpass filter and the first mixer. This double balanced mixer, fed by the first local oscillator ($f_{LO1}$ = 153.56 MHz) performs the frequency up-conversion of the 13.56 MHz input signal, which is the first IF of the entire testbed, to the second IF at 140 MHz. At the second IF a 5 MHz SAW (surface acoustic wave) bandpass filter is followed by a variable gain amplifier which is used to set the desired transmit power level. The output of this amplifier is filtered and fed into the second mixer which performs the second frequency up-conversion to the UHF band. The output frequency is determined by the second LO, which is centered at $f_{LO2}$ = 1006.5 MHz. By tuning the LO2 frequency the transmit frequency can be chosen in the range of 865 MHz to 868 MHz. This range is determined by a SAW bandpass filter following the second mixer. An identical filter is also used after a two stage amplifier providing an output power of 20 dBm sufficient to drive an external power amplifier. A directional coupler is implemented to provide a sample of the transmit signal to an onboard power detector and for the CCU. For flexibility this directional coupler circuit is doubled and can be used in combination with the external power amplifier. Hence the system may be used with different power amplifiers or even without an external power amplifier. Figure 5 shows a picture of the UHF transmitter implemented.

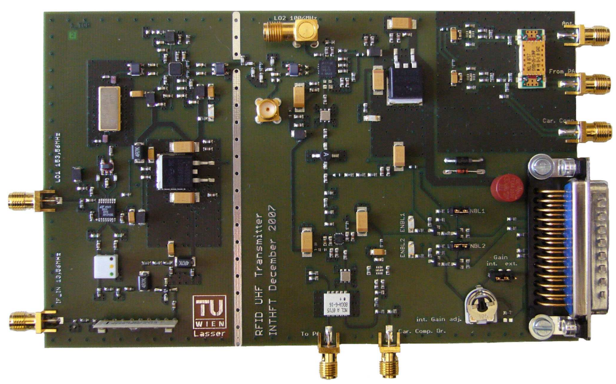


**Fig. 5.** UHF Transmitter

### 3.3 Receiver

At the receiver input both the backscattered signal from the tag and the self-interfering signal caused by the transmitter are superposed. The sources of the interference depend on the configuration of the frontend [12]. If the frontend is operated with a single antenna for transmitting and receiving usually a circulator separate, transmit and receive signals. The antenna mismatch and the isolation of the circulator are then causing the crosstalk. If separate transmit and receive antennas are used, the receive antenna will directly receive a fraction of the transmitted signal. Figure 6 shows a simplified block diagram of the receiver where the signals are first bandpass filtered with an SAW filter and then immediately the reduction of the carrier crosstalk is performed.

A directional coupler inserts the phase shifted and amplitude matched carrier compensation signal, provided by the CCU, to suppress most of the leaking carrier. The recovered signal is then amplified with a low noise amplifier (LNA). At this point of the signal chain a small part of the signal is picked up by a directional coupler for power monitoring and for control of the CCU. One main goal of the receiver design was to achieve immunity to high input power levels, mainly caused by self-interference, while maintaining a low noise figure. Therefore, several methods of adjusting the gain of the different receiver subsections

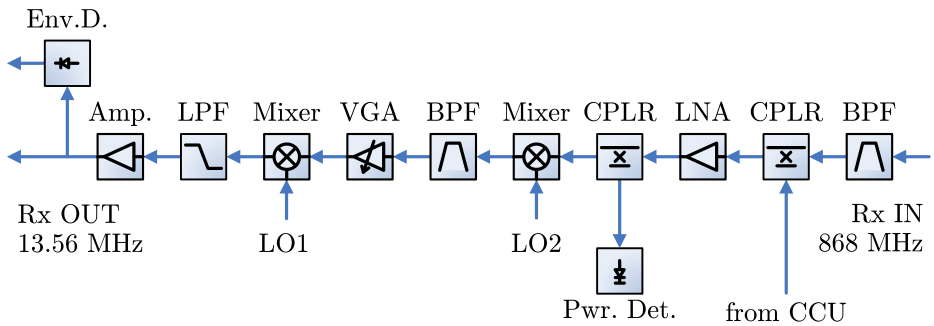


**Fig. 6.** Simplified block diagram of the UHF receiver

were implemented. To improve the noise figure when high carrier suppression is realized a second amplifier can be switched into the signal chain at the UHF stage. After carrier compensation the signal is frequency converted to the first receiver IF at 140 MHz with a doubly balanced mixer, and filtered again. The receiver bandwidth of 5 MHz is determined by the SAW bandpass filter. This filter is followed by a variable gain amplifier, which has an adjustable gain range of 23 dB. Gain can be set digitally in 1 dB steps. Right after the variable gain amplifier the signal power is monitored by a power detector circuit. The amplified IF signal is fed into the second receiver mixer, which performs the frequency conversion down to 13.56 MHz. The mixer is followed by a lowpass filter to suppress undesired mixing products. After the last amplifier the receiver output level is sufficient to drive the ADC on the rapid prototyping board. This last amplifier further provides decoupling from the receiver output and the lowpass filter. Additionally an envelope demodulator is implemented and its separate output can be used for direct oscilloscope display in certain measurement scenarios. The noise figure of the receiver depends on the gain settings and can vary between 5 dB and 16 dB. Figure 7 shows the UHF receiver implemented.

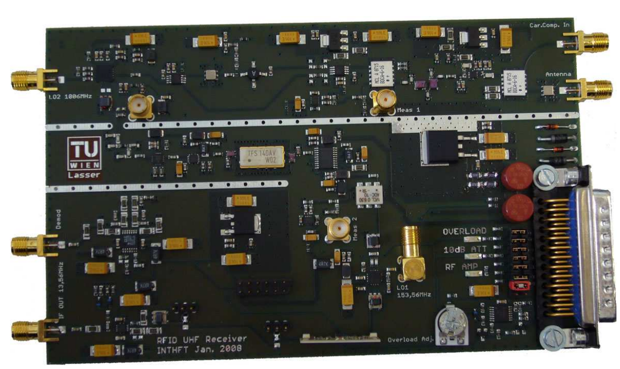

**Fig. 7.** UHF Receiver

### 3.4 Carrier Compensation Unit

Figure 8 depicts the block diagram of the CCU which consists of a vector modulator and a fixed gain amplifier. A small part of the transmit signal, provided by the

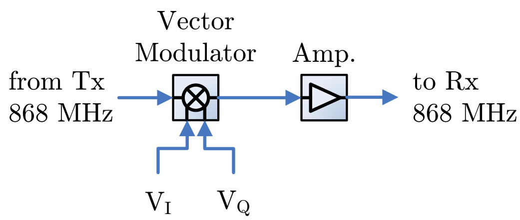


**Fig. 8.** Simplified block diagram of the CCU.

transmitter at a special CCU port, is directly fed into the vector modulator. The vector modulator enables a true 360° adjustable phase and an adjustable amplitude range of 30 dB of the incoming signal. It has two input lines, for adjusting the magnitude of the inphase and of the quadrature components, respectively. To compensate the coupler losses (at transmitter and as well as receiver) and enable cancelation of strong leaking carrier signals, the vector modulator is followed by an amplifier with a high 1 dB compression point of 27 dBm. The output signal of the CCU is fed via a directional coupler into the receiver. For optimum carrier cancelation the leaking carrier, present at the receiver, and the cancelation signal, provided by the CCU, should have equal amplitude but a phase shift of 180°. Manual adjustment of the CCU is possible in rather static scenarios. Otherwise the adjustment of the CCU is managed by a microcontroller. Figure 9 shows the carrier compensation unit implemented. Measurements of the perfor-

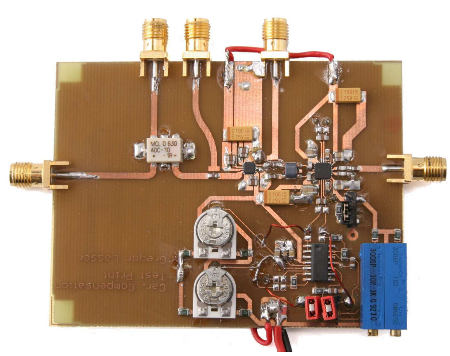

**Fig. 9.** Carrier Compensation Unit

mance of the CCU with a network analyzer show a leaking carrier suppression of up to 65 dB. This ultimate value was measured in a wired scenario and will not be fully achieved in real open scenarios with moving scatterers.

## 4 Verification Measurement

For verification of the frontend a typical RFID scenario with a commercially available RFID tag was chosen. As the signal source for the UHF transmitter at 13.56 MHz a vector signal generator (VSG) was used. The VSG was programmed to transmit a query command as specified in the EPC global standard. Two signal generators were used as local oscillators and connected via power dividers to the corresponding LO-ports of the transmitter and the receiver. The LO1 frequency was set to 153.56 MHz and the LO2 frequency was set to 1006 MHz. This results in a communication frequency of 866 MHz. The external power amplifier provides a gain of 25 dB and a maximum output power of 35 dBm. The transmit power was adjusted manually by means of the variable gain amplifier of the transmitter. Power was measured after the circulator with a power meter connected to the system via an external directional coupler. The isolation performance of the circulator was degraded by the return loss of 15 dB of the circularly polarized patch antenna used in this experiment. To become more independent of the antenna an impedance tuner was used to improve the impedance matching of the antenna. Both output signals of the receiver have been monitored using an oscilloscope. Figure 10 shows a block diagram of the measurement setup. In a

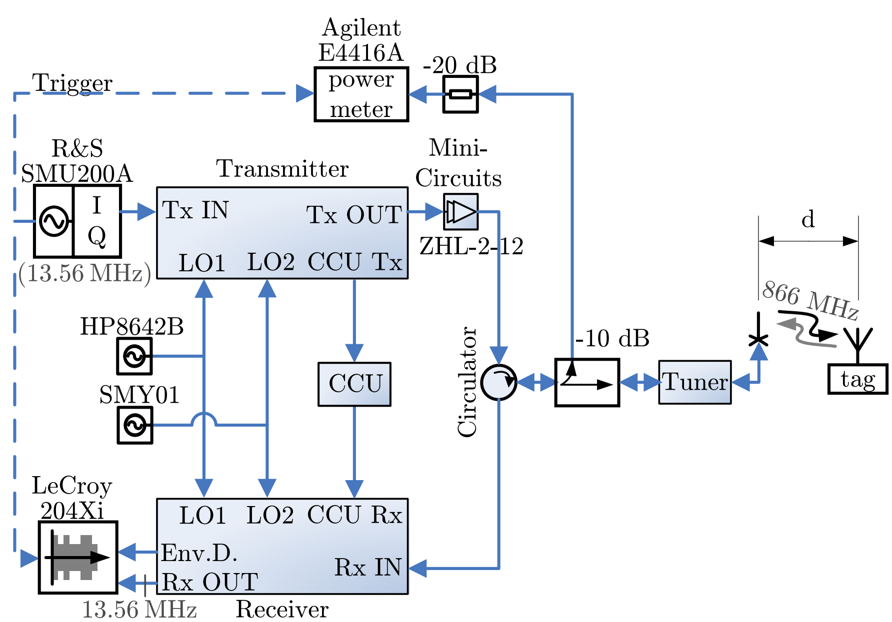


**Fig. 10.** Measurement Setup

first step the transmitter-receiver isolation was optimized by means of the tuner at a medium output power of 20 dBm. After this the output power of the power amplifier was set to 33 dBm and the isolation was optimized with the carrier compensation unit in a second step. Both optimizations have been performed without the tag. The losses of the antenna cable, the directional coupler, and the tuner, and finally the antenna gain of 5 dBi (for linear polarization) result in a transmit power of 33 dBm ERP (effective radiated power). The transponder chosen for this verification measurement was a Rafsec G2 tag which was fixed onto a wooden ladder. Figure 11 shows the measurement scenario at a corridor of our institute. In front of the picture the transmit antenna connected to the


**Fig. 11.** Measurement scenario

UHF frontend can be seen while the wooden ladder with the tag is located at the end of the corridor. The maximum distance between reader and tag where we could observe a tag answer at the envelope detector output was d=11 m. The corresponding screenshot of the oscilloscope for this measurement is given in Figure 12. The upper trace (channel 1) of the screenshot shows the frequency downconverted tag answer at the 13.56 MHz output of the receiver and the lower trace (channel 3) shows the output of the envelope detector of the receiver. For this measurement the carrier compensation was adjusted manually.

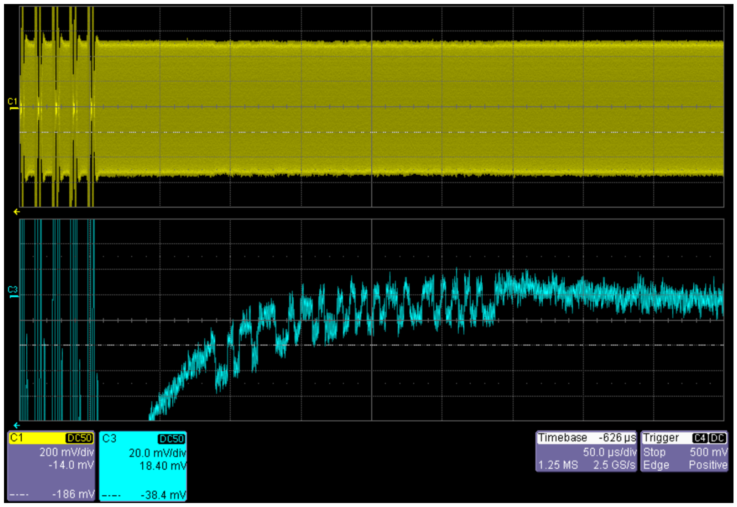


**Fig. 12.** Received tag answer in a corridor: read distance 11 m

## 5 Summary

In this paper we presented a UHF reader frontend designed and implemented for a flexible RFID testbed. The frontend consists of a transmitter, a receiver and an additional carrier compensation unit which allows for a significant reduction of the self-interference at the receiver. The design allows standard compliant experiments as well as standard independent experiments in the field of RFID. The frontend allows a multitude of configurations and shows very good performance. A read range of about 11 m was obtained using a commercially available passive RFID transponder. The flexibility and modularity of the frontend allow for numerous measurement scenarios and make it capable to handle future trends and extensions.

## Acknowledgment

This work has been funded by the Christian Doppler Laboratory for Design Methodology of Signal Processing Algorithms.

## References

1. Finkenzeller, K.: RFID Handbook: Fundamentials and Applications in Contactless Smart Cards and Identification, 2nd ed. John Wiley& Sons, Inc. (2003)
2. Stockman, H.: Communication by Means of Reflected Power. In: Proceedings of the IRE, vol.36, no.10, pp. 1196-1204, (1948)
3. Angerer, C., Knerr, B., Holzer, M., Adalan, A., Rupp, M.: Flexible Simulation and Prototyping for RFID Designs. In: RFID 2007, The first international EURASIP Workshop on RFID Technology, Book of Proceedings, p. 51-54, (2007)

4. Meindl-Pfeiffer, G., Kloibhofer, R., Kaltenberger, F., Humer, G.: Multi-Standard Development and Measuring Platform for MIMO-Software Defined Radio. In: Proceedings of the EUSIPCO, Antalya, Turkey, Sept. 2005, invited.
5. EPCGlobal: EPC Global HF Version 2, document Version 0.3. January 2007.
6. EPCGlobal: EPC Radio-Frequency Identity Prototcols Class-1 Generation-2 UHF RFID Protocol for Communications at 860 MH - 960 MHz, Version 1.2.0 (2007)
7. ISO / IEC: ISO / IEC 15693, Identification Cards - Contactless Integrated Circuit Cards - Vicinity Cards. January 2000.
8. Angerer, C.: A Digital Receiver Architecture for RFID Readers. In: SIES 2008, Third International Symposium on Industrial Embedded Systems. Montpellier, France, 2008.
9. Knerr, B., Holzer, M., Angerer, C., Rupp, M.: Slot-by-slot maximum likelihood estimation of tag populations in framed slotted aloha protocols. In: Proceedings of International Symposium on Performance Evaluation of Computer and Telecommunication Systems (SPECTS), Edinburgh, UK, 2008.
10. Curty, J.P., Declercq, M., Dehollain, C., Joehl, N.: Design and Optimization of Passive UHF RFID Systems. Springer Science+Business Media, LLC (2007)
11. Langwieser, R., Fischer, M., Scholtz, A.L., Rupp, M., Humer, G.: Rapid Prototyping for RF-Transmitters and Receivers. In: Communication Systems and Networks 2006., ACTA Press (2006)
12. Penttilä, K., Sydänheimo, L. and Kivikoski, M.: Implementation of Tx/Rx isolation in an RFID reader. In: Int. J. Radio Frequency Identification Technology and Applications, vol. 1, No. 1, pp.7489. (2006)